ETH zürich

ETH Library

Recent Trends in Advanced Photoinitiators for Vat Photopolymerization 3D Printing

Review Article

Author(s):
Bao, Yinyin

Publication date:
2022-07

Permanent link:
https://doi.org/10.3929/ethz-b-000551481

Rights / license:
Creative Commons Attribution 4.0 International

Originally published in:
Macromolecular Rapid Communications 43(14), https://doi.org/10.1002/marc.202200202

Funding acknowledgement:
177178 - 3D printing manufacturing of patient-tailored drug releasing stents (SNF)
190313 - Enhancing the Red Emission of Perylene Diimide in Solid or Aggregated State by Simple Polymerization (SNF)

This page was generated automatically upon download from the ETH Zurich Research Collection.
For more information, please consult the Terms of use.

Macromolecular Rapid Communications
www.mrc-journal.de

Recent Trends in Advanced Photoinitiators for Vat Photopolymerization 3D Printing

Yinyin Bao

3D printing has revolutionized the way of manufacturing with a huge impact on various fields, in particular biomedicine. Vat photopolymerization-based 3D printing techniques such as stereolithography (SLA) and digital light processing (DLP) attract considerable attention owing to their superior print resolution, relatively high speed, low cost, and flexibility in resin material design. As one key element of the SLA/DLP resin, photoinitiators or photoinitiating systems have experienced significant development in recent years, in parallel with the exploration of 3D printing (macro)monomers. The design of new photoinitiating systems cannot only offer faster 3D printing speed and enable low-energy visible light fabrication, but also can bring new functions to the 3D printed products and even generate new printing methods in combination with advanced optics. This review evaluates recent trends in the development and application of advanced photoinitiators and photoinitiating systems for vat photopolymerization 3D printing, with a wide range of small molecules, polymers, and nanoassemblies involved. Personal perspectives on the current limitations and future directions are eventually provided.

1. Introduction

Since last decade, 3D printing (also called additive manufacturing) has brought enormous opportunities for rapid production of complex architectures and experienced exponential growth in both techniques and materials.[1–3] As a chemical process-based 3D printing technique, vat photopolymerization possesses remarkable advantages, such as flexible material design, high print resolution, fast printing, and smooth print surface.[4–6] As most commonly used vat photopolymerization methods, stereolithography (SLA),[7,8] digital light processing (DLP),[9,10] and continuous liquid interface production (CLIP)[11,12] have shown wide potential in customized fabrication of tissue scaffolds,[13,14] medical devices,[15,16] soft robots,[17,18] dental implants,[19,20] microfluidic devices[21,22] and drug delivery systems.[6,23]

SLA and DLP usually rely on the layer-by-layer solidification of a liquid resin containing (macro)monomers that can be photocrosslinked under light irradiation in the presence of a photoinitiator.[7,8] With a digital micromirror device, DLP can more efficiently generate 2D light shapes than SLA (**Figure 1**A,B). On the other hand, CLIP enabled continuous fabrication with much higher speed by introducing an oxygen-permeable window to form a dead zone of photopolymerization at the bottom of the resin (Figure 1C). Recently, emerging techniques such as tomographic[24–26] or linear volumetric printing[27] completely revoked the layer stepping process in vertical direction (Figure 1D,E), and further push the boundaries of photopolymerization 3D printing in terms of speed, resolution and material scope.

Photopolymerization has a long-standing history in the field of photochemistry. Due to its great advantages such as solvent-free and energy-efficient processes, photopolymerization has been widely applied in coating industry, painting/printing inks, adhesives, and dentistry.[28a,b] Photopolymerization is considered as a chain polymerization process initiated by ionic or radical species generated by light irradiation of a photoinitiator or photoinitiating systems.[28c,d] When successive layers of photopolymerized materials are stacked to form a controlled 3D structure thanks to the computer-aided design and precision light engineering, photopolymerization transforms into 3D printing. To enable fast photopolymerization and hence high-quality 3D printing, the photoinitiator should have an adequately high molar extinction coefficient at the light source wavelength and generate active initiating species (e.g., free radicals) under excitation by photons.[5] In recent years, a large amount of photoinitiators or photoinitiating systems for 3D printing have been reported with high efficiency, with some of them working in the visible light range and thus compatible with the commercial 3D printers using 405 nm light-emitting diodes (LED).[29–31] To facilitate the application of photopolymerization 3D printing in biomedical applications, the development of visible light photoinitiators beyond 405 nm that can use low-energy visible LEDs would be highly desired but much less reported.[32] On the other hand, photoresponsive

Y. Bao
Institute of Pharmaceutical Sciences
Department of Chemistry and Applied Biosciences
ETH Zurich, Vladimir-Prelog-Weg 3, Zurich 8093, Switzerland
E-mail: yinyin.bao@pharma.ethz.ch

The ORCID identification number(s) for the author(s) of this article can be found under https://doi.org/10.1002/marc.202200202

© 2022 The Authors. Macromolecular Rapid Communications published by Wiley-VCH GmbH. This is an open access article under the terms of the Creative Commons Attribution License, which permits use, distribution and reproduction in any medium, provided the original work is properly cited.

DOI: 10.1002/marc.202200202

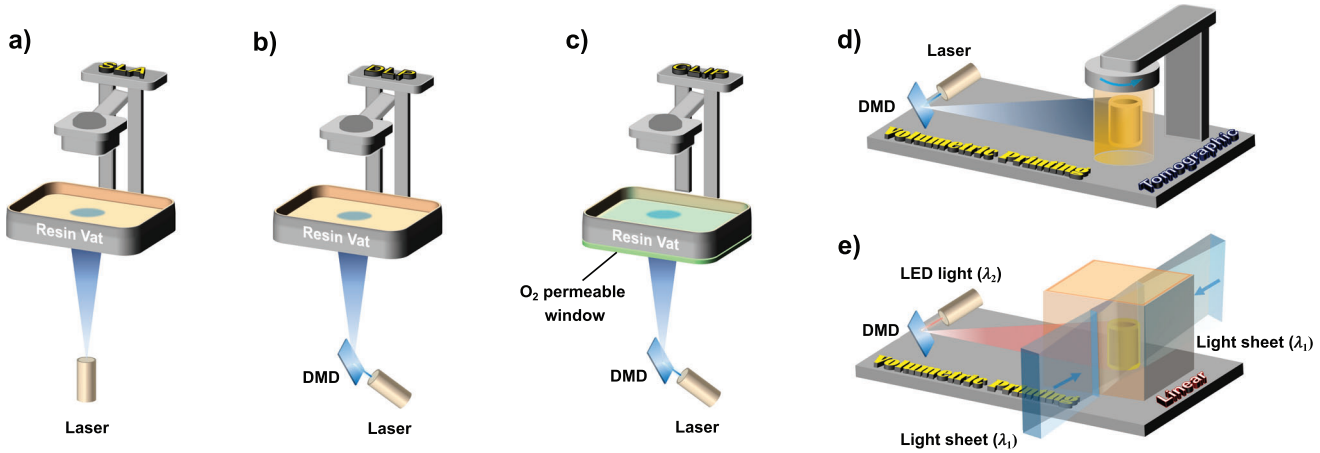

Figure 1. Representative vat photopolymerization 3D printing techniques using photoinitiators. A) SLA; B) DLP; C) CLIP; D) Tomographic volumetric printing. Adapted with permission.[25] Copyright 2019, the American Association for the Advancement of Science (AAAS). E) Linear volumetric printing. Adapted with permission.[27] Copyright 2020, Springer Nature.

molecules such as molecular photoswitchs[33] or reversible addition–fragmentation chain-transfer (RAFT) agents[34] have been introduced to vat photopolymerization for functional 3D printings. In addition to small molecules, photoinitiating polymers[35,36] and nanoassemblies[37,38] have been designed to benefit the additive manufacturing of sustainable materials, biodegradable elastomers, biocompatible hydrogels, etc.

In this work, instead of providing a comprehensive summary of photoinitiators used in 3D printing, we focus on these recently emerging trends in the development and application of advanced photoinitiators or photoinitiating systems for vat photopolymerization 3D printing mainly in last three years. The 3D printing systems and applications are discussed with a perspective on current limitations and future research directions eventually provided. The readers can refer to recently published review articles[29–31] for more thorough overview of the visible light photoinitiators.

2. Low Molecular Weight Photoinitiating Systems

As one of the two most important elements of a photopolymerization system, photoinitiator directly undergoes chemical reactions upon light irradiation. Dependent on the specific photoinduced reactions, different types of photoinitiators involving one or more components have been designed. In general, the photoinitiation process can be achieved in two different ways: i) the photoinitiator undergoes a home-cleavage to produce free radicals after light absorption (type I photoinitiator) and ii) noncleavable molecules generate free radicals with hydrogen abstraction from hydrogen donors as co-initiators (type II photoinitiator).[29] The commonly used commercial photoinitiators are usually type I photoinitiators, such as 2,4,6-trimethylbenzoyldiphenyl phosphine oxide (TPO, **Figure 2**) and phenylbis(2,4,6-trimethylbenzoyl)phosphine oxide (BAPO, or Omnicure 819, previously known as Irgacure 819, Figure 2),[30,39,40] which have been extensively applied in SLA and DLP printing with both UV light and 405 nm LED. Recently, the emerge of photoredox catalysts enabled the development of highly efficient photoinitiating systems that can be activated by low-energy irradiation, and thus applicable with green-to-near infrared (NIR) light.[32] Both metal complexes (e.g., zinc tetraphenylporphyrin, ZnTPP,[41]) and organic dyes (e.g., eosin Y,[42] Figure 2) have been discovered as photoredox catalysts that can react with reducing or oxidizing agents at excited states, resulting in electron transfer and generation of radicals or ion species.[29,43–45] This system has most recently shown great potential in visible light 3D printing, which may facilitate the biomedical applications of vat photopolymerization, especially for the production of tissue constructs, drug formulations and medical implants.

2.1. Visible Light Photoinitiators beyond 405 nm

Although the commercial photoinitiators like TPO and BAPO have maximum molar extinction coefficient below 400 nm, their absorption spectra still cover the violet light region. Therefore, they are compatible with the commercial SLA and DLP printers using 405 nm LED, benefiting from their highly efficient photon absorption. On the other hand, despite numerous newly synthesized visible light photoinitiators (e.g., Ivocerin,[46] NDP2[47a] and TPA-DTP,[47b] Figure 2), they were rarely tested for 3D printing under light irradiation beyond 405 nm. In this section, we focus on the commercial or synthetic visible light photoinitiators that have been used in vat photopolymerization with light of relatively longer wavelength, such as green, red, white or even NIR irradiation.

As a commercially available dye and biocompatible photoinitiator, eosin Y can be activated by green light and used in bioprinting.[48,49] Kim and co-workers reported the first cell-attachable SLA bioink containing gelatin methacryloyl (GelMA) and eosin Y.[42] As shown in **Figure 3**A, patterned cell-laden hydrogels were printed using commercial projector beam light covering whole visible light range (400–700 nm) and the cells can well proliferate inside the hydrogels to form 3D intercellular networks.

Tris(2,2′-bipyridyl)dichloro-ruthenium(II), or $Ru(bpy)_3^{2+}$ is a metal complex-based visible light photoinitiator.[50,51] Recently, Zhang and co-workers demonstrated that the camera light of

 © 2022 The Authors. Macromolecular Rapid Communications published by Wiley-VCH GmbH

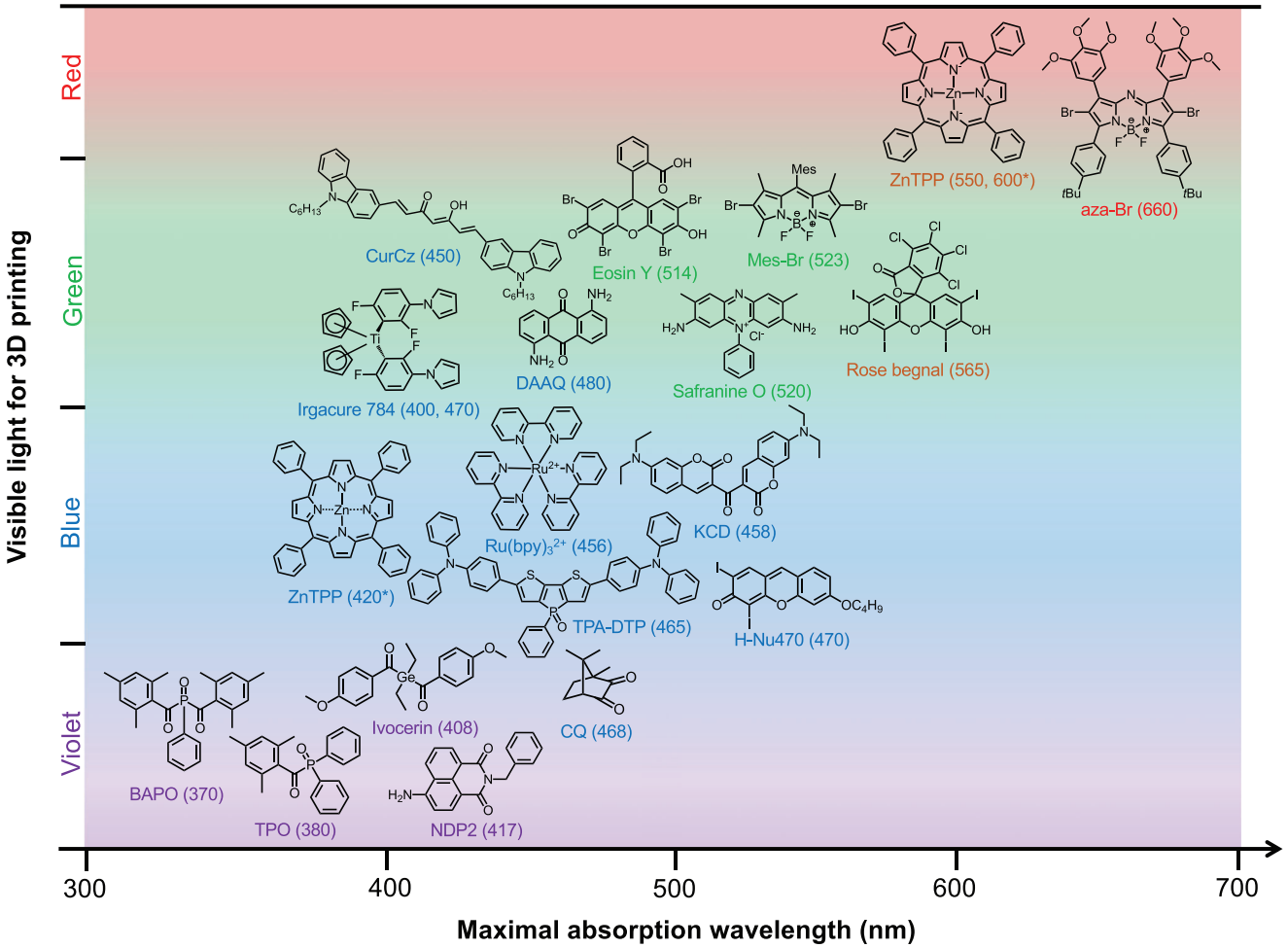

Figure 2. Visible light photoinitiators for photopolymerization 3D printing using violet to red light irradiation: BAPO (Omnicure 819),[46] TPO,[39b] Ivocerin,[46] NDP2,[47a] CQ,[54] ZnTPP,[32,41] $Ru(bpy)_3^{2+}$,[50–52] TPA-DTP,[47]b H-Nu470,[32] KCD,[59] Irgacure 784,[54] DAAQ,[55a,b] CurCz,[55c] safranine O,[58] eosin Y,[42,48,49] Mes-Br,[56] rose bengal,[32] aza-Br.[56] *ZnTPP has two absorption bands locating at blue and yellow color region, respectively.

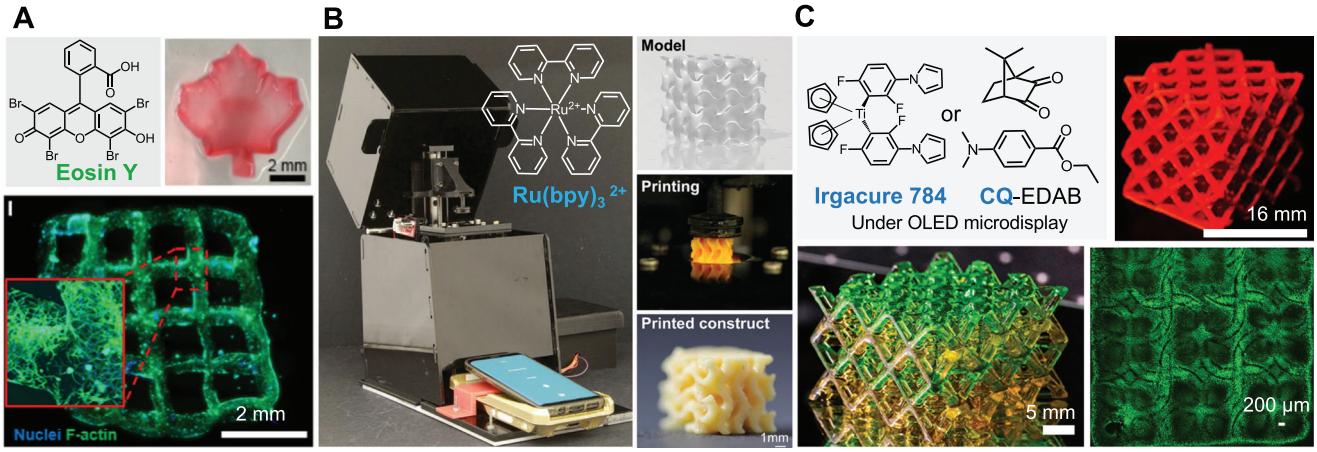

Figure 3. Commercial photoinitiators for visible light 3D printing. A) Eosin Y-based SLA printing of GelMA bioink and cell-laden hydrogels. Reproduced with permission.[42] Copyright 2018, American Chemical Society. B) $Ru(bpy)_3^{2+}$-based smartphone-enabled DLP printing of complex constructs from PEGDA 575. Reproduced with permission.[52] Copyright 2021, Wiley-VCH GmbH. C) Irgacure 784- and CQ-EDAB-based OLED-modulated DLP printing of lattice structure, multimaterial layers and hydrogel scaffold for cell attachment from PEGDA 700 resins. Reproduced with permission under the terms of the Creative Commons License.[54] Copyright 2021, the Author(s), published by Cell Press.

 © 2022 The Authors. Macromolecular Rapid Communications published by Wiley-VCH GmbH

smartphone enabled efficient 3D printing of commercial photopolymers using $Ru(bpy)_3^{2+}$ hexahydrate with sodium persulfate on a portable DLP printer[52] (Figure 3B). A series of complex structures as well as hydrogel tissue analogs were successfully fabricated from polyethylene glycol diacrylate (PEGDA) 575 or GelMA solutions. The authors anticipated this smartphone-powered DLP printing strategy could be highly useful for the fabrication of point-of-care medical implants and cell-laden tissues in situ, especially in resource-limited situations. At the same time, Goyanes et al. reported another smartphone-enabled 3D printing system using the same $Ru(bpy)_3^{2+}$ photoinitiator.[53] Warfarin-loaded tablets of various sizes and tailored shapes were printed from PEGDA 575 with high dimensional precision, and sustained release characteristics were observed. This study expanded the scope of point-of-care manufacturing of personalized drug formulations.

Fang and co-workers recently reported another visible light 3D printing platform using an organic light-emitting diode (OLED) microdisplay with two different well-established photoinitiating systems involved, that are Irgacure 784 (type I) and camphorquinone (CQ)-ethyl 4-dimethylaminobenzoate (EDAB) (type II).[54] This visible light OLED-modulated digital platform offered scalable printing of commercial resins, PEGDA photopolymers and bioactive hydrogels while being simple and low-costly. In addition, multimaterial printing was also achieved with excellent resolution and complex architectures, by incorporating an air jet set for resin exchange (Figure 3C).

In addition to the commercial photoinitiators, the exploration of tricomponent photosystems based on a photoredox catalyst together with electron donor/acceptor pair has brought new opportunities for 3D printing with visible light, in particular green light.[55] Page and co-workers evaluated the photopolymerization kinetics of isobornyl acrylate using a series of mesityl-functionalized boron-dipyrromethene (BODIPY) dyes under a green LED light at 530 nm.[56] Only 0.1 mol% dye molecule was used for resin preparation with 0.1 mol % donor 2-(butyryloxy)-N,N,N-trimethylethan-1-aminium butyltriphenylborate, and 1.0 mol % acceptor [4-(octyloxy)phenyl](phenyl)iodonium hexafluoroantimonate (diphenyliodonium). By using an attenuated total reflectance (ATR)-Fourier transform infrared spectroscopy (FTIR) spectroscopy, it is revealed that the monomer conversion reached maximum value (≈80%) after only 8.5 and 6.5 s for brominated and iodinated BODIPYs (Mes-Br and Mes-I), respectively (**Figure 4**A). The green LED light intensity was as low as 0.44 mW cm^{-2}, which is much less intense than commercial DLP light resource (≈20 mW cm^{-2}).

The authors found that the high photopolymerization rate was due to the halogenation-induced efficient intersystem cross (ISC) of the dyes from S_1 to T_1 state under photoexcitation, which resulted in longer lifetime of the excited state.[56] Using Mes-Br system, they realized rapid 3D printing of a hierarchical octet-tuss lattice structure by DLP with 530 nm green LED (≈1.8 mW cm^{-2}) (Figure 4A). A BODIPY derivative (aza-Br) with red light absorption (660 nm) was also synthesized and maximum conversion was achieved in 11.4 s using the same system under 740 nm far-red LED light at 16.0 mW cm^{-2}. This rapid far-red or NIR light-triggered photopolymerization was unprecedented.

The same group also developed tricomponent photosystems using 5,7-diiodo-3-butoxy-6-fluorone (H-Nu470), rose bengal, and ZnTPP, respectively.[32] Based on similar donor/acceptor co-initiators, rapid photocuring of the resins containing dimethyl acrylamide and trimetylolpropane triacrylate was achieved with blue (≈460 nm), green (≈525 nm), or red (≈615 nm) light using the corresponding dye. This is comparable with the conventional BAPO photoinitiator under violet light (405 nm), while the concentration of the dyes was only 0.1–0.3 wt% versus 0.5 wt% for BAPO. The highly efficient photopolymerization enabled rapid high-resolution 3D printing by a DLP system with blue, green, and red LEDs, respectively (Figure 4B). Most recently, Page group further employed a cyanine 7 derivative called H-Nu 815, which even pushed the 3D printing light scope to NIR region. It was demonstrated that 3D architectures could be fabricated by invisible light (≈850 nm) with a low intensity (<5 mW cm^{-2}).[57]

Allonas and co-workers developed another tricomponent photosystem using safranine O with green light absorption in combination of tetraphenylborate salt as electron donor and 2-(4-methoxyphenyl)-4,6-bis(trichloromethyl)-1,3,5-triazine (TA) as electron acceptor (Figure 4C).[58] The photopolymerization kinetics of a resin containing ethoxylated bisphenol A diacrylate and 0.1 wt% safranine O was evaluated under green laser irradiation (532 nm). The tricomponent system showed much higher polymerization rate compared to the bicomponent systems using either dye/donor or dye/acceptor (conversion 57.3% vs 9.9% and 1.5% in 20 s) at light intensity of ≈50 mW cm^{-2}. Increasing the dye concentration to 0.4% allowed high-resolution printing of an Eiffel tower model by a DLP printer with a polychromatic Xenon arc lamp covering full visible spectrum, at a layer exposure time of 5 s.

Using the same TA acceptor, Xie and co-workers prepared a bicomponent photosystem using commercially available 3,3'-carbonylbis(7-diethylaminocoumarin) (KCD) regarding its high ISC efficiency up to 92%.[59] The photooxidation of KCD by TA could produce the initiating radical ($TA^{\bullet}$) for rapid photopolymerization and a deethylated product (i.e., KCD_2) which can confine the light penetration due to its high absorption coefficient at 448 nm (4.3×10^4 L mol^{-1} cm^{-1}). On the other hand, if photoreduced by N-phenylglycine, the generated amino-alkyl radical and ketyl radical result in a significant blueshift of the absorption (≈61 nm) compared with KCD (Figure 4D). The photooxidation of KCD (≈3×10^{-3} M) enabled high print fidelity upon visible light irradiation using a digital light projector covering 420–780 nm. This is indicated by the high-resolution 3D printed objects from a monomer mixture composed of N,N-dimethylacrylamide, trimethylolpropane ethoxylate triacrylate, and pentaerythritol tetraacrylate (Figure 4D, inset). The minimal feature with 20 μm in height and 23 μm (1 pixel) in width could be achieved at a light intensity of 60 mW cm^{-2}.

From the chemical structure of the photoinitiators or photosensitizers discussed in this section, we can see there are two general ways to push their absorption to longer wavelength: i) to design large π-conjugated structure such as conjugated macrocycle (e.g., ZnTPP[41]), spirocyclic dye (e.g., eosin Y[42]) and extended linear molecule by cross-coupling (e.g., CurCz[55c]); and ii) to introduce electron-donating and electron-accepting substituents to generate intramolecular charge transfer (e.g., Mes-Br and aza-Br[56]). This is consistent with the general principle for chemical design of organic dye molecules but with additional requirement for the efficient phototriggered cleavage or redox reaction.

 © 2022 The Authors. Macromolecular Rapid Communications published by Wiley-VCH GmbH

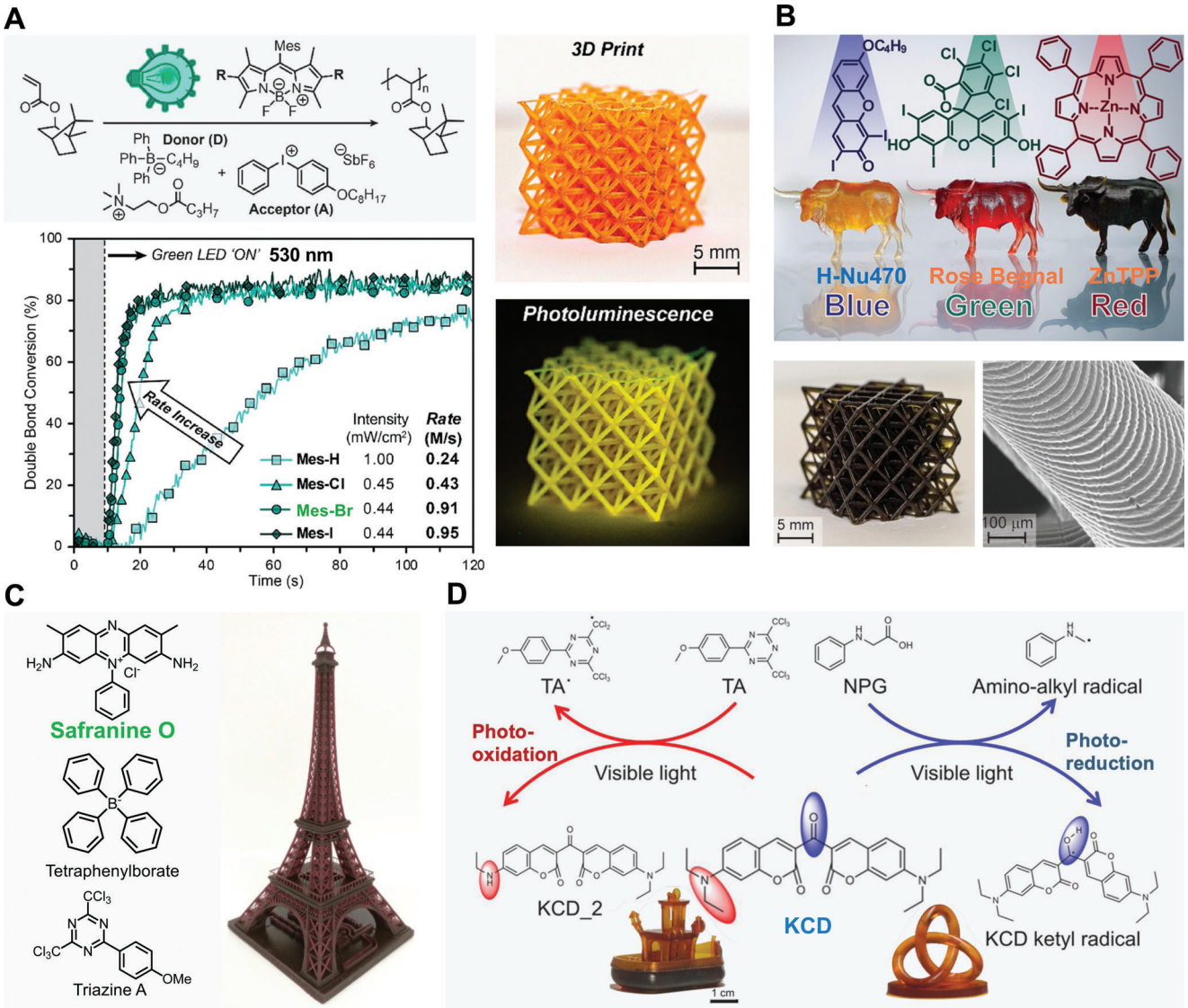

Figure 4. Emerging photoinitiating systems for visible light 3D printing. A) Mesityl BODIPY dye-based photoinitiating systems (top left), its double bond conversion versus irradiation time (bottom left) and green LED light 3D printed lattice structure (right). Reproduced with permission.[56] Copyright 2020, American Chemical Society. B) H-Nu470, rose bengal, and ZnTPP for 3D printing with blue, green, and red light, and the 3D printed lattice structure based on ZnTPP system. Reproduced with permission under the terms of the Creative Commons License.[32] Copyright 2020, the Author(s), published by American Chemical Society. C) Safranine-based photoinitiating system and the 3D printed Eiffel tower model. Reproduced with permission.[58] Copyright 2019, Wiley-VCH GmbH. D) KCD-based photoredox processes and the 3D printed boat and knot models. Reproduced with permission under the terms of the Creative Commons License.[59] Copyright 2021, the Author(s), published by Springer Nature.

2.2. RAFT Photoinitiating System

In parallel, the introduction of RAFT agents (e.g., trithiocarbonate) to 3D printing resins has attracted increasing attention due to the post-printing transformation enabled by reactivation.[34,60] Jin and co-workers reported the first visible light 3D printing via photo-RAFT polymerization at 405 nm (**Figure 5**A).[60] Using a trithiocarbonate-based iniferter (e.g., 4-cyano-4-[(dodecylsulfanylthiocarbonyl) sulfanyl] pentanoic acid, CDTPA, or dibenzyl trithiocarbonate, DBTTC), PEGDA 250 or tetra(ethylene glycol) diacrylate (TEGDA) can be printed by DLP. "RAFT" letters have been fabricated using a low-intensity violet LED (1.8 mW cm^{-2}). Despite the relatively long exposure time (>8 min for each layer), this strategy allowed controlled attachment of functional moieties on the 3D printed object surface. Furthermore, they designed a photoinduced electron/energy transfer-RAFT (PET-RAFT) system by incorporating an organic dye (e.g., erythrosin B[34] or eosin Y[61]), which greatly accelerated the photopolymerization with maximum conversion reached in 2–5 min (Figure 5B,C). Subsequently, DLP printing with green light (525 nm, 4.3 mW cm^{-2}) was realized with exposure time of 20–30 s. This system also offered an opportunity to design 4D printed materials by controlling the spatially resolved light doses.[34] As claimed by the authors, the inclusion of RAFT agent

© 2022 The Authors. Macromolecular Rapid Communications published by Wiley-VCH GmbH

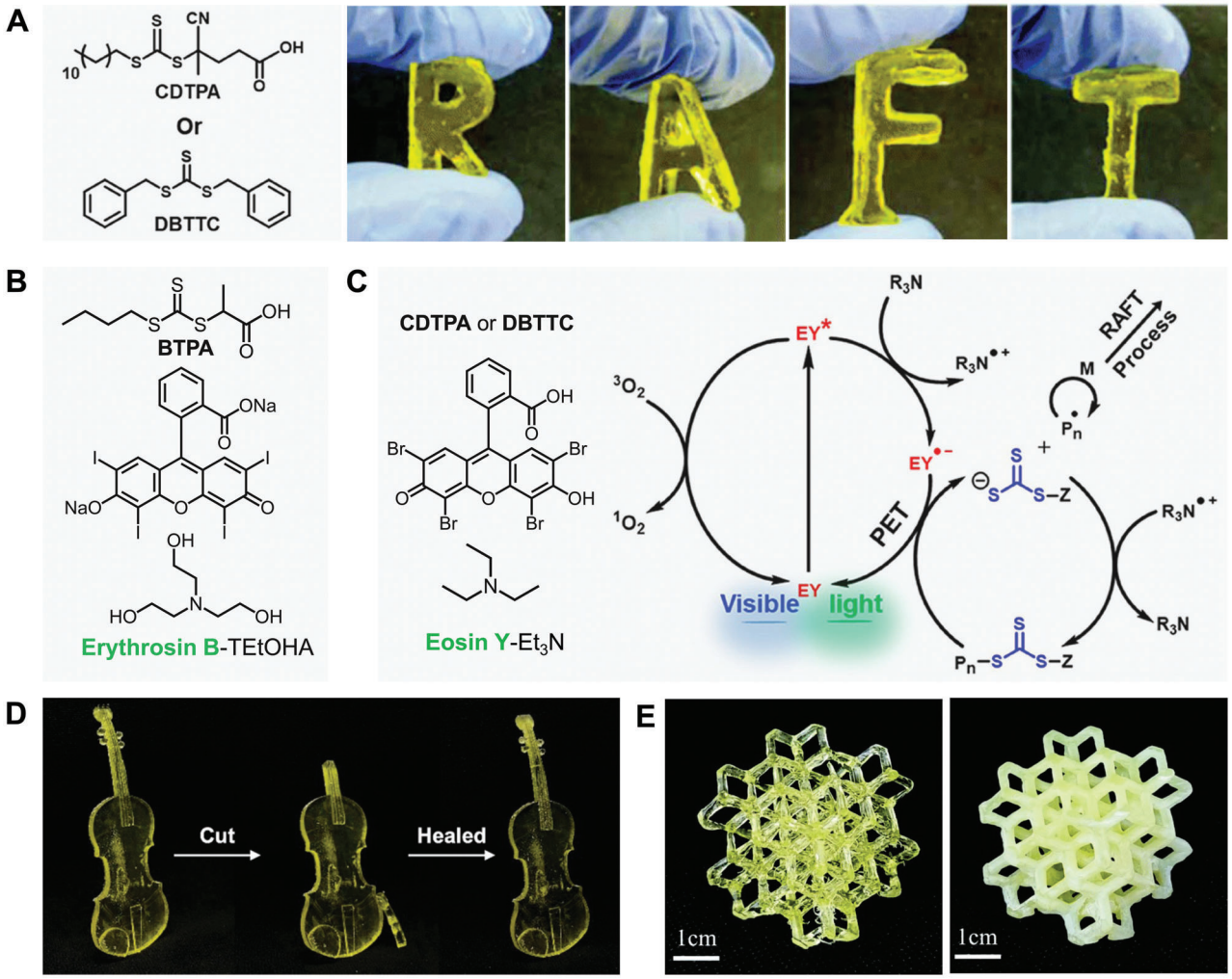

Figure 5. RAFT systems for visible light 3D printing. A) Trithiocarbonate-based photoiniferters and the 3D printed "RAFT" letters. Reproduced with permission.[60] Copyright 2020, Royal Society of Chemistry. B) Erythrosin B-based PET-RAFT system for green light 3D printing. Reproduced with permission.[34] Copyright 2019, Wiley-VCH GmbH. C) Eosin Y-based PET-RAFT system for green light 3D printing and the photoredox processes. Reproduced with permission.[61] Copyright 2020, American Chemical Society. D) Self-healing 3D printed violin model based on DBTTC-TPO system. Reproduced with permission under the terms of the Creative Commons License.[63] Copyright 2021, the Author(s), Wiley-VCH GmbH. E) 3D printed lattice structure using RAFT resin (left) or RAFT-silica nanoparticle resin (10 wt% silica, right) based on methyl 2-(*n*-butylthiocarbonothioylthio) propanoate (MBTP)-TPO system. Reproduced with permission.[64] Copyright 2022, Royal Society of Chemistry.

in the photopolymerization resin allowed the 3D printed materials to be postfunctionalized with the residue active moieties, and this strategy can potentially provide control over the mechanical properties of 3D printed products due to the more regularly organized networks formed by controlled radical polymerization.

The addition of commercial photoinitiator (e.g., BAPO or TPO) to RAFT system could significantly improve the printing speed and resolution, while maintaining the postfunctionalization activity.[62] Interestingly, self-healing 3D printed objects could be fabricated from a RAFT resin containing 2-hydroxyethyl acrylate and ethylene glycol dimethacrylate using DBTTC (1.5 mol%) and TPO (0.75 mol%) as coinitiators (Figure 5D).[63] Furthermore, Boyer group demonstrated that RAFT 3D printing can be used for silica/polymer composite fabrication (Figure 5E)[64] as well as micro- to nanoscale structure control in 3D printed complex objects.[65]

Recently, Jin and co-workers explored the possibility of RAFT 3D printing under red LED light (635 nm, 0.5 mW cm^{-2}) by introducing ZnTPP to the resin, with a disk-shaped model printed.[66] Meanwhile, Zhu and co-workers attempted cationic RAFT polymerization toward NIR light 3D printing by using a commercially available iron catalyst, cyclopentadienyl iron dicarbonyl dimer ($Fe_2(Cp)_2(CO)_4$) as the photocatalyst.[67] Although further optimization is required, photomediated RAFT system[45] has broadened the scope of additive manufacturing in a living manner.[68]

2.3. Functional Photoswitches

The photoswitch-incorporated photoinitiating systems represent another important trend in photopolymerization 3D printing. With light-triggered isomerization offering tunable functions in

 © 2022 The Authors. Macromolecular Rapid Communications published by Wiley-VCH GmbH

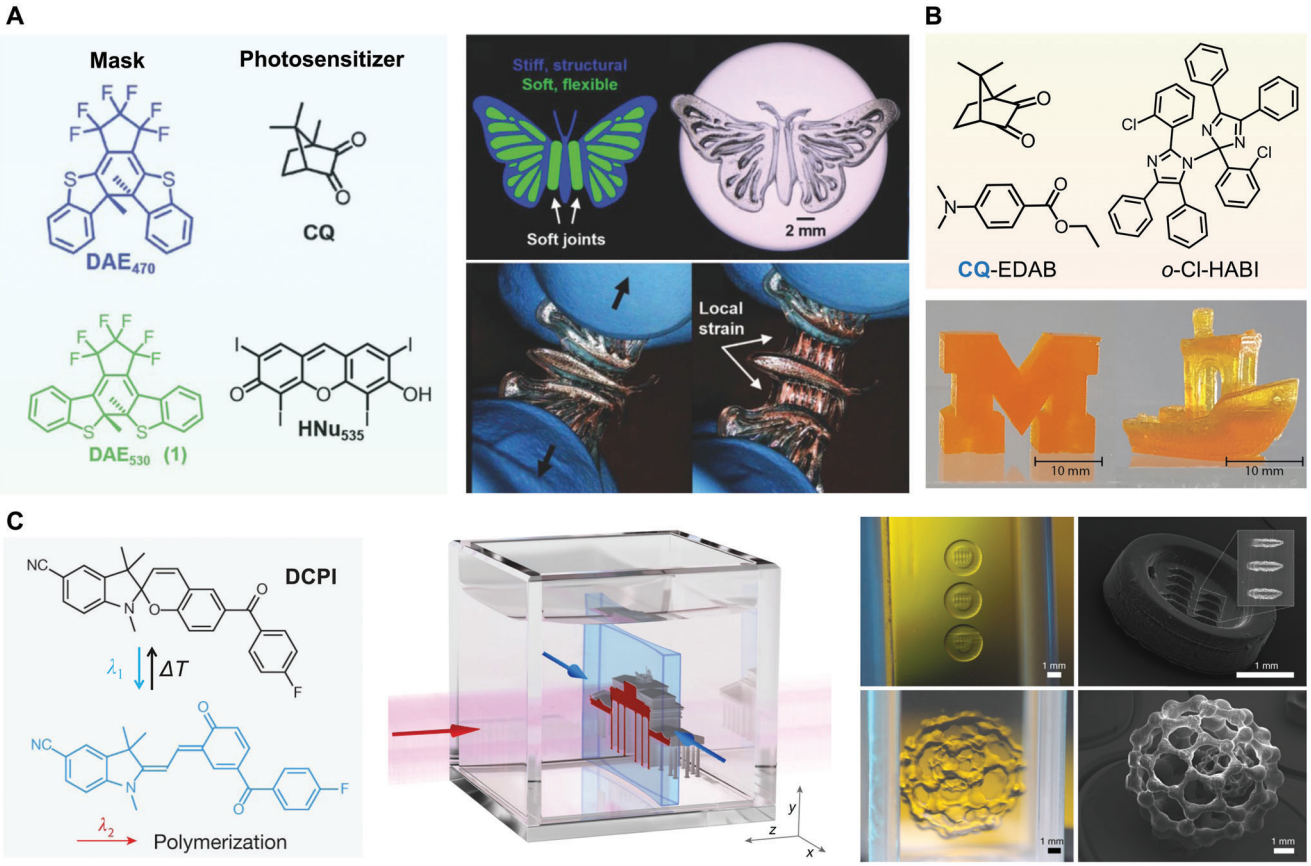

Figure 6. Photoswitches for functional 3D printing. A) Liquid mask photoswitches with corresponding photoinitiators, and multimaterial 3D printed butterfly specimen with soft joints. Reproduced with permission under the terms of the Creative Commons License.[33] Copyright 2018, the Author(s), Wiley-VCH GmbH. B) Photoinhibitor (*o*-Cl-HABI)-photoinitiator (CQ-EDAB) system and the volumetric 3D printed solid block M and tug boat model. Reproduced with permission under the terms of the Creative Commons License.[73] Copyright 2019, the Author(s), published by AAAS. C) Bifunctional photoswitch DCPI for dual-color volumetric printing and the 3D printed test plate and nested fullerene molecular model with scanning electron microscope (SEM) images. Reproduced with permission under the terms of the Creative Commons License.[27] Copyright 2020, the Author(s), published by Springer Nature.

3D microstructures,[69–71] photoswitches have been employed for multimaterial vat photopolymerization[33,72] and volumetric printing.[27,73,74] Hawker and co-workers reported the first one-step multimaterial 3D printing using photochromic molecules which can control polymerization through coherent bleaching fronts.[33] As shown in **Figure 6**A, two different diarylethene photoswitches, 1,2-bis(2-methyl-1-benzothiophen-3-yl) perfluorocyclopentene (DAE_{530}) and 1,2-bis(3-methyl-1-benzothiophen-2-yl)perfluorocyclopentene (DAE_{470}), were used as the solution masks for CQ and a xanthene green light absorbing dye HNu_{535}. In this way, when mixed with both epoxy- and acrylate-based monomers, the photoswitch-photoinitiator system allowed selective photocuring by controlling the exposure to blue (470 nm) or green light (530). This is because the blue exposure led to dual radical and cationic curing, while green exposure only caused radical crosslinking, so that 3D objects with spatially resolved chemical and mechanical domains can be directly fabricated by wavelength-selective printing (Figure 6A). This so-called solution mask liquid lithography (SMaLL) realized multimaterial 3D printing from one single-resin. Later on, dual-wavelength DLP was also employed for multilateral printing of epoxy-acrylate resin using UV (365 nm) and visible light (full spectrum).[75] Despite the good spatial control, the printing resolution was less satisfying in the absence of functional photoswitches.

The dual wavelength was also used to achieve volumetric printing that does not rely on layer-by-layer stacking for conventional vat photopolymerization.[27,73,74] Scott and co-workers introduced bis[2-(ochlorophenyl)-4,5-diphenylimidazole] (*o*-Cl-HABI) as a photoinhibitor to the CQ-EDAB photoinitiating system.[73] Under 365 nm UV irradiation, *o*-Cl-HABI can generate lophyl radicals rapidly recombining with propagating carbon-centered radicals and thus inhibit the photopolymerization. On the other hand, when irradiated with visible light (470 nm), *o*-Cl-HABI is almost transparent while CQ-EDAB can efficiently initiate the phtopolymerization due to the strong absorption. Consequently, concurrent photoinitiation and photoinhibition can be achieved using two-color light with variable intensity. It allowed single step volumetric fabrication of complex objects. This technique enabled rapid 3D printing by overcoming the time-consuming layer-stacking steps (Figure 6B).

On the other hand, in combination of a dual-function photoswitch and light-sheet technology, Hecht and co-workers

 © 2022 The Authors. Macromolecular Rapid Communications published by Wiley-VCH GmbH

developed a linear volumetric printing approach for rapid high-resolution manufacturing.[27] By attaching a benzophenone type II photoinitiator into a spiropyran photoswitch molecule, a dual-color photoinitiator (DCPI) was synthesized with both photoswitching and photoinitiating activities. Absorbing UV light at 375 nm, DCPI can switch to the latent merocyanine state, which has a broad absorption covering 450–700 nm. In the presence of a coinitiator (e.g., triethanolamine), the switched DCPI can generate the excited benzophenone moiety under red light irradiation (e.g., 585 nm), and initiate the photopolymerization of acrylate monomers (e.g., pentaerythritol tetraacrylate, PETA). Importantly, the photoswitch will come back to the initial state by thermal relaxation to the ground state, if not exposed to the visible light. As shown in Figure 6C, by intersecting light beams of different wavelengths for linear excitation, local polymerization inside a confined monomer volume can be achieved, resulting in high-speed 3D printing with better resolution compared to tomographic volumetric printing (25 µm vs 80 µm).[25–27]

3. Polymeric Photoinitiators

In addition to small molecule-based photoinitiating systems, polymeric photoinitiators or macrophotoinitiators recently appeared for functional photopolymerization 3D printing. Usually by covalent linkage of photoinitiating groups to a polymer chain either by polymerization or postfunctionalization, the initiator–polymer conjugates can be easily obtained.[44,76] This strategy can improve the biocompatibility and solubility of the molecular photoinitiators while reduce the migration of the photolysis byproducts.[36,76] Owing to the requirement of hydrogel fabrication for biomedical applications, the development of water-soluble photoinitiators is highly important.[31b] Compared to hydrophobic photoinitiators, water-soluble photoinitiators for 3D printing are relatively less reported, especially for visible light ones.[77] In addition to the type II photoinitiators such as eosin-Y[42] and riboflavin,[77b] TPO- and BAPO-based organic salts have been designed as the representative water-soluble photoinitiators.[31b,77c–e] Employing a different strategy, Grützmacher and co-workers synthesized a water-soluble macrophotoinitiator by attaching BAPO group to a PEG oligomer (950 g mol^{-1}) via one-pot reaction (**Figure 7**A).[35a] The resulted BAPO-PEG exhibited higher molar extinction coefficients in the visible region (390–430 nm) in water compared to BAPO salt-based photoinitiators, BAPO-ONa and BAPO-OLi. Based on 50 wt% PEGDA 700 aqueous formulation, the authors found that BAPO-PEG offered much faster photopolymerization under 460 nm LED light, with $t_{95\%}$ of 53 s versus 76 and 70 s for the salts. At a concentration of 0.7 wt%, BAPO-PEG enabled high-resolution DLP printing of a well-defined gyroid structure. This work opened new perspectives on the visible light photopolymerization 3D printing of complex hydrogel structures using macrophotoinitiators.

As a wood-derived natural product, lignin is one of the most abundant biopolymers on earth.[78] Its phenolic structure allows chemical modification to introduce functional groups for either photoinitiation or polymerization.[79] Zhao and co-workers explored the intrinsic photoinitiating ability of dealkaline lignin (DAL) for 3D printing owing to its ketyl and phenoxyl moieties that can generate free radicals under light irradiation (Figure 7B).[80] By derivatization with long alkane or alkene chains onto the DAL backbone, the resulted two products DAL-11ene and DAL-12ane showed improved solubility. Using 1,6-hexanediol diacrylate as the monomer, both derivatives facilitated the photopolymerization with double bond conversion twice of the value for DAL within same time. With EDAB as the coinitiator and 10 wt% DMSO as the solvent, the system can reach maximal conversion in ≈2 min at 0.5 wt% of DAL-11ene or DAL-12ane. Despite their absorption in UV region (e.g., maximal peak at 280 nm), visible light DLP 3D printing was realized using 1,6-hexanediol diacrylate and the lignin photoinitiator (1 wt%) with a 405 nm LED and relatively high exposure time (60 s). Importantly, the cytocompatibility of the 3D printed products was evaluated on murine L929 fibroblast cells by live/dead staining and the cells incubated with 3D printed tablets showed comparable viability to the negative control. This work represents a good example using sustainable polymers for high-value product development.

To also overcome the solubility or compatibility issue of molecular photoinitiator (e.g., BAPO) for solvent-free 3D printing, we recently synthesized BAPO-conjugated polyesters by ring-opening polymerization of D,L-lactide (DLLA) and ϵ-caprolactone (CL) initiated by hydroxyl BAPO molecules.[36] The random copolymerization can convert the solid BAPO molecules to liquid macrophotoinitiators (BAPO-poly(DLLA-*co*-CL)), and thus enabled the solvent-free resin preparation that is desired for 3D printing of biodegradable elastomers.[15,81] The macrophotoinitiators showed slightly lower molar extinction coefficient but with a red-shift to the longer wavelength compared to the commercial BAPO photoinitiator (Figure 7C). By using a series of biodegradable macromonomers with similar chemical structures (poly(DLLA-*co*-CL methacrylate)) and varied molecular weight, high-resolution DLP printing of biodegradable elastomers with tunable mechanical properties was achieved. The macrophotoinitiators are well compatible with different types of 3D printing monomers (e.g., PEGDA), and shape-memory devices can also be fabricated based on the semicrystalline polycaprolactone dimethacrylate.

Chiappone, Grützmacher and co-workers attached BAPO to another type of biopolymer, γ- cyclodextrin, and simultaneously introduced acrylate groups to the platform, resulted in enhanced crosslinking ability.[82,83] The macrophotoinitiator named BAPO-γ-cyclodextrin showed almost ten times higher molar extinction coefficient than commercial BAPO and thus enabled ultrahigh polymerization rate. BAPO-γ-cyclodextrin was used as a photoinitiator and also a crosslinker for the DLP printing of monofunctional monomers, 2-hydroxyethyl methacrylate (HEMA) and poly(ethylene glycol methyl ether methacrylate) (PEGMEMA). Stabilized by thermoreversible hydrogen bonding interactions, the 3D printed products exhibited excellent thermally triggered shape memory response with strain recovery of 99% (Figure 7D). In addition to conventional macrophotoinitiators, hybrid composites[84] and charge transfer complexes[85] have also been designed for improving the performance of vat photopolymerization 3D printing. Furthermore, this strategy was also found valuable in two-photo polymerization for microstructure fabrication.[86]

 © 2022 The Authors. Macromolecular Rapid Communications published by Wiley-VCH GmbH

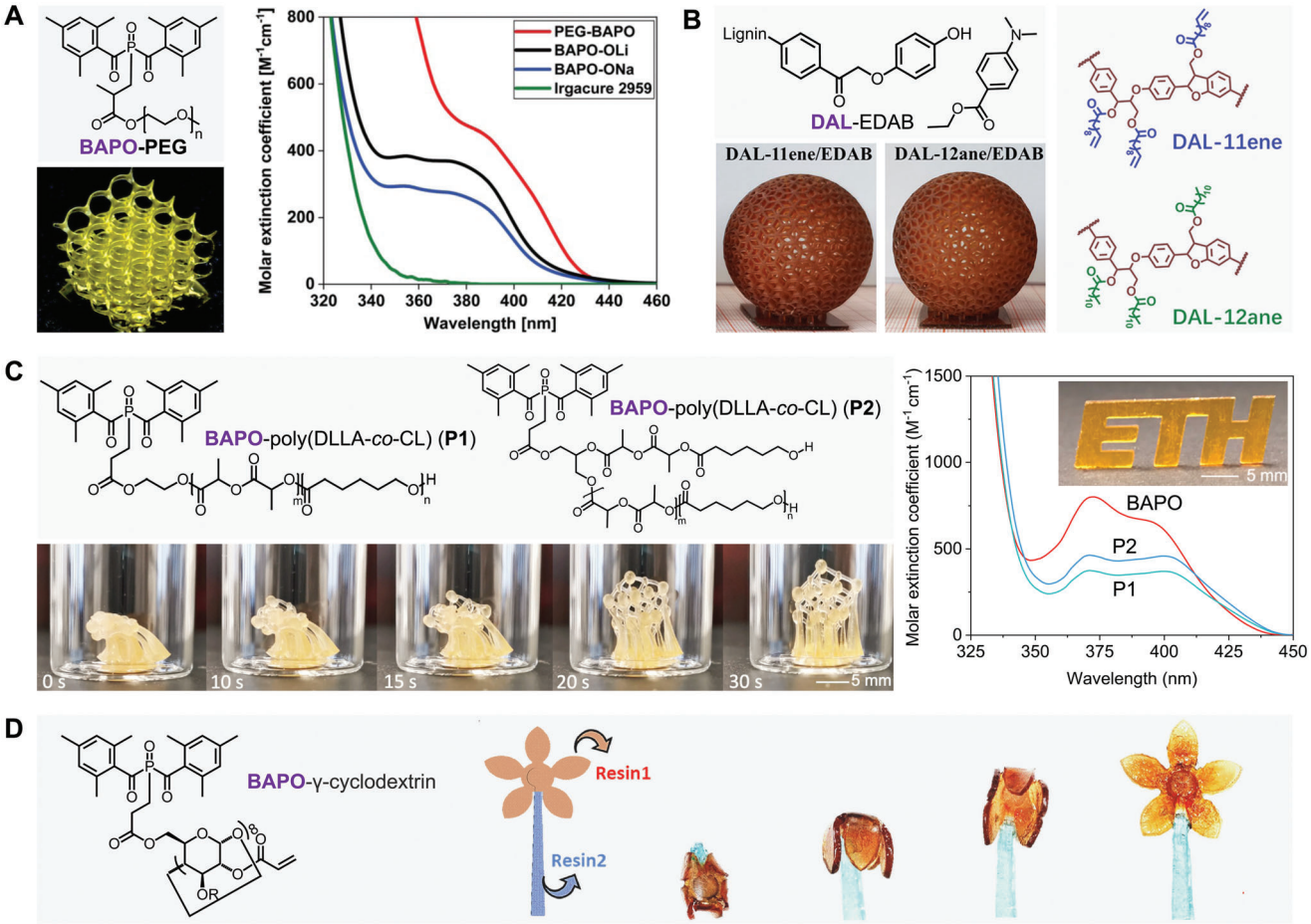

Figure 7. Polymeric photoinitiators for vat photopolymerization. A) BAPO-PEG structure (left top), its absorption spectrum compared to other water-soluble photoinitiators (right) and 3D printed gyroid hydrogel structure (left bottom). Reproduced with permission.[35a] Copyright 2018, Royal Society of Chemistry. B) Lignin-based photoinitiating system and the 3D printed hollow spheres. Reproduced with permission.[83] Copyright 2020, American Chemical Society. C) BAPO-poly(DLLA-*co*-LA)s (left top), their absorption spectra compared to BAPO (right), and 3D printed biodegradable shape-memory NaCl crystal lattice model (left bottom). Inset: 3D printed ETH logo. Reproduced with permission under the terms of the Creative Commons License.[36] Copyright 2021, the Author(s), published by American Chemical Society. D) BAPO-γ-cyclodextrin and the 3D printed shape memory flower model. Reproduced with permission.[83] Copyright 2021, Elsevier Ltd.

4. Nanoassemblies as Photoinitiators

Nanotechnology has become a pivotal tool in the development of novel therapeutic and diagnostic medical systems.[87–89] Recently, its alliance with 3D printing brought new opportunities for the advance of multifunctional customized medical devices and pharmaceutical products.[90] For example, nanoformulation of commercial hydrophobic photoinitiator enabled the 3D printing in aqueous solutions without the need of tedious synthetic procedures.[37] As a commonly used commercial photoinitiator with good thermal and shelf stability, TPO has high molar extinction coefficient (300 to 800 M^{-1} cm^{-1}) with absorption spectrum extending up to 420–440 nm.[91] However, its low water solubility limited the application of TPO (similar to BAPO) in hydrogel fabrication and further biomedical applications. Magdassi and co-workers prepared water-dispersible TPO nanoparticles by spray drying of volatile microemulsions, and up to 3 wt% TPO can be dispersed in water which is 100 times higher than that of bulk TPO molecule.[37] The TPO nanoparticles preserved strong UV absorption in water with molar extinction coefficient of 218 M^{-1} cm^{-1} at 365 nm. Using an aqueous ink containing acrylamide (38.5 wt%) and ethoxylated trimethylolpropane triacrylate (8.9 wt%), a woodpile-structured hydrogel scaffold was printed by SLA at a TPO concentration of 2.4% (**Figure 8**A).

Later on, the same group discovered another nanoparticular system enabling rapid photopolymerization in aqueous solutions, however, with no conventional molecular photoinitiators incorporated.[92,93] The system was based on a semiconductor–metal hybrid structure made from cadmium sulfide (CdS) nanorods with gold tips. Unlike conventional photoinitiators, the CdS–Au nanorods can produce hydroxyl radicals while simultaneously scavenging oxygen to generate additional superoxide and hydroxyl radicals.[93] As a result, the molar extinction coefficient is four orders of magnitude larger than BAPO- and TPO-based salts ($\approx 10^7$ vs ≈ 250 M^{-1} cm^{-1}).[94] As shown in Figure 8B, a spherical C180 buckyball hydrogel model (73 wt% water) was successfully printed by a DLP printer from acrylamide-PEGDA ink with a tiny amount of CdS–Au nanorods (0.5×10^{-6} M). Recently, CdSe

© 2022 The Authors. Macromolecular Rapid Communications published by Wiley-VCH GmbH

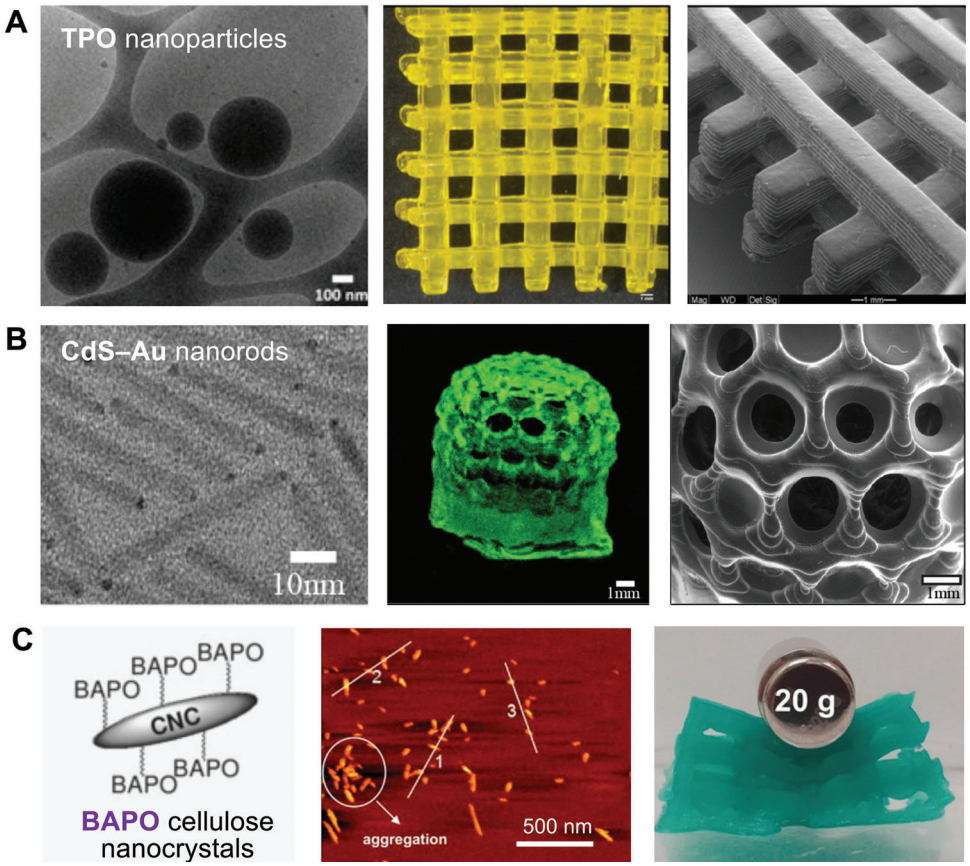

Figure 8. Nanoassemblies as photoinitiators for vat photopolymerization. A) Cryogenic transmission electron microscopy (cryo-TEM) image of TPO nanoparticles (left), photograph of 3D printed woodpile hydrogel structure (middle) and the SEM image (right). Reproduced with permission under the terms of the Creative Commons License.[37] Copyright 2016, the Author(s), published by AAAS. B) TEM image of CdS–Au nanorods (left), photograph of 3D printed Buckyball hydrogel structure under UV irradiation (middle) and the SEM image of the dried structure. Reproduced with permission.[93] with permission. Copyright 2017, American Chemical Society. C) Illustration of BAPO-cellulose nanocrystals (left), AFM image (middle) and the 3D printed cubic-lattice hydrogel structure after swelling for 1 h. Reproduced with permission.[38] Copyright 2018, Wiley-VCH GmbH.

quantum dots[95] and carbon dots[96] were also explored as visible light photoinitiators for hydrogel 3D printing, due to their respective photoredox catalytic properties.

Compared to inorganic nanoparticles, naturally occurring nanomaterials are more biocompatible and sustainable with potential biomedical applications.[97a] As a unique type of nanomaterials, cellulose nanocrystals are derived from the most abundant natural polymer, cellulose. Grützmacher and co-workers proposed a strategy to develop highly efficient nanophotoinitiators by surface immobilization of cellulose nanocrystals with BAPO groups.[38] By elemental analysis, it was found that about 2100 BAPO groups were bound to one single nanocrystal, and the morphology of cellulose nanocrystals was maintained with slight aggregation. Based on 50 wt% PEGMEMA aqueous ink, the BAPO nanocrystals offered faster photopolymerization kinetics compared to BAPO-ONa, with a gelation time twice as short. Using BAPO nanocrystals (6.14 wt%) as both a photoinitiator and crosslinker, the 3D printed hydrogel from PEGMEMA showed higher mechanical modulus than the BAPO nanocrystal-free hydrogels, despite the high swelling ratio in water. This facile surface modification with BAPO moieties may become a general strategy for the functionalization of various nanomaterials and thus 3D printing of nanocomposites.[97b]

Another type of nanoassembiles used in photopolymerization 3D printing is upconversion nanoparticles (UCNPs), owing to their capability in converting NIR light excitation into visible and ultraviolet emission, which can be further used for photolithography.[98,99] Different from other nanoformulations that were used to enhance the initiation/crosslinking efficiency or to improve the solubility/compatibility of the photoinitiators, UCNPs were employed to achieve vat photopolymerization under NIR light irradiation with conventional UV or blue light photoinitiators. It is well known that two-photon polymerization allows volumetric printing without the layer-by-layer stacking manner for SLA or DLP. This is because the photopolymerization can only occur at the focal point of a laser beam benefiting from the nonlinear light absorption of a photoinitiator under high-intensity laser radiation. However, the femtosecond NIR laser required for two-photon polymerization has limited print size and speed (voxel size ≈100 nm) while being much more expensive than conventional LED, which made its wide application like SLA or DLP difficult.[100,101]

 © 2022 The Authors. Macromolecular Rapid Communications published by Wiley-VCH GmbH

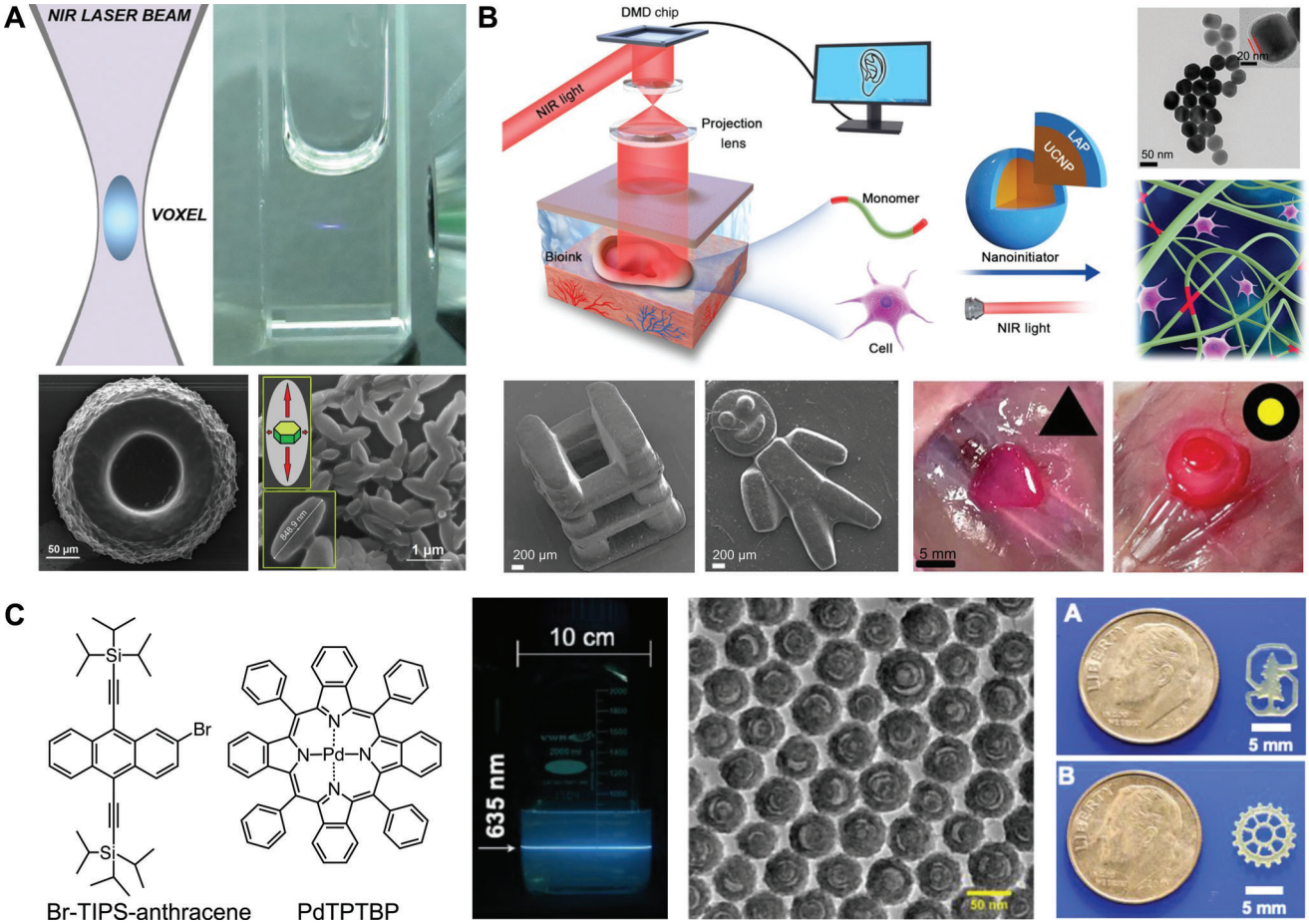

Figure 9. Upconversion nanoparticle-assisted 3D printing. A) Luminescent voxel formation in a cuvette containing photocurable resin and $NaYF_4$-based UCNPs under NIR light illumination (top), SEM image of 3D printed microstructure (bottom left) and SEM image of rice-like structures formed when the UCNP concentration is below the threshold (bottom right). Reproduced with permission under the terms of the Creative Commons License.[100] Copyright 2018, the Author(s), published by Springer Nature. B) Schematic diagram of UCNP@LAP-based noninvasive 3D bioprinting (top), SEM images of 3D printed constructs (bottom left) and noninvasive in vivo printed vitamin B12-stained triangle and two-layer cake-like constructs (bottom right). Inset: TEM image of UCNP@LAP nanoinitiator. Reproduced with permission under the terms of the Creative Commons License.[105] Copyright 2020, the Author(s), published by AAAS. C) Chemical structures of annihilator (Br-TIPS-anthracene) and sensitizer (PdTPTBP), the upconversion light beam excited by 645 nm red light imaged through a 600 nm shortpass filter (left), TEM of the upconversion nanocapsules (middle) and 3D printed Stanford logo and gear (right). Reproduced with permission under the terms of the Creative Commons License.[101] Copyright 2021, the Author(s), published by Elsevier.

To combine the advantages of two-photopolymerization and vat photopolymerization, Khaydukov and co-workers reported the high-resolution NIR light 3D printing assisted by UCNPs,[100] following the pioneering studies about upconversion photolithography.[99,102–104] Inorganic UCNPs with a core/shell structure (β-$NaYF_4$:Yb^{3+},Tm^{3+}/$NaYF_4$) were synthesized as an internal NIR-triggered UV source inside the photocurable resin thanks to the deep penetration of NIR light.[103] Under 975 nm laser irradiation at 15 W cm^{-2}, the nanoparticles can emit UV fluorescence at 288, 345, and 360 nm, which overlapped with the absorption of commercial photoinitiators such as TPO. By mixing the nanoparticles with photocurable resin in a cuvette, a voxel structure similar to that generated by two-photon excitation can be formed by the NIR irradiation (**Figure 9**A). Using a commercial resin containing TPO as the photoinitiator, a model microstructure was fabricated with NIR laser at 7 W cm^{-2} and scanning speed of 0.2 mm s^{-1}. It was found that rice-like microparticles instead of continuous structure were formed when the UCNP concentration was below a threshold, likely due to the heterogeneous distribution of emission intensity around the nanoparticle. To enable the formation of geometrically connected phases growing from nanoparticle surfaces, the minimum nanoparticle concentration was calculated to be 16.8 mg mL^{-1}. The authors envisaged this strategy could be translatable for the applications in biomedicine such as tissue bioprinting.

Subsequently, Gou and co-workers realized noninvasive in vivo 3D bioprinting using an UCNP coated with UV/blue-light photoinitiator lithium phenyl-2,4,6-trimethylbenzoylphosphinate (LAP, Figure 9B).[105] Upon 980-nm excitation (power 1.5–3.5 W) the UCNP@LAP nanoinitiator showed upconversion emission located at 345 and 361 nm, which can be further absorbed by LAP. Using a GelMA solution (15 wt%), 3D hydrogel structures can be printed with 1 wt% UCNP@LAP and exposure time of 15 s. This process was further evaluated in vivo by subcutaneously

 © 2022 The Authors. Macromolecular Rapid Communications published by Wiley-VCH GmbH

injecting 50 µL of a precursor solution into the BALB/c mice. By hematoxylin and eosin (H&E) staining of tissues surrounded to the printed hydrogel constructs, the surrounding tissues did not show significant inflammation and abnormal defects in 7 d after printing, indicating the biocompatibility of the 3D printed products. Moreover, customized living construct was fabricated in vivo by this noninvasive technique using an ink containing adipose-derived stem cells, and applied to tissue defect repair. After 10 d, the 3D printing treatment group showed significant improvement in wound closure compared to the control. Therefore, together with other 3D printing techniques,[106,107] the potential of UCNP-assisted NIR light photopolymerization has been witnessed in biomedical applications. Recently, upconversion photopolymerization has also been introduced to CLIP system.[108]

Despite these promising results, the challenges in upconversion-assisted vat photopolymerization remain. For example, high power density is required for inorganic UCNPs, and the nanoparticle synthesis can be challenging to scale, which may limit the versatility of this technique for wide applications.[101] Most recently, Congreve and co-workers reported a volumetric printing strategy using triplet fusion upconversion nanocapsules.[101] It is based on the photopolymerization at a focal point driven by triplet-triplet-annihilation, through nanoencapsulation of photon upconversion solution within a silica shell decorated with PEG. Instead of using inorganic nanoparticles, triisopropylsilyl ethynyl anthracene (TIPS-anthracene) and palladium (II) meso-tetraphenyl tetrabenzoporphine (PdTPTBP) were selected as the annihilator and sensitizer, respectively, for the preparation of upconversion nanosystems (Figure 9C). Based on the TIPS-anthracene resin containing PETA as the monomer and Ivocerin as the photoinitiator, a Stanford logo and a gear were successfully printed in 8 min using a 625 nm LED at 78 mW cm^{-2}. The minimal print feature can reach 50 µm at a power density of 224 mW cm^{-2}. This approach is particularly useful for the 3D printing of highly viscous resins as it does not reply on the layer-by-layer stacking. But still, high nanocapsule loading (15 wt%) is needed to ensure the maximal upconversion efficiency.

5. Conclusion and Perspectives

In parallel with the advances of photocuring techniques and monomers, significant progress in the development and application of advanced photoinitiators for vat photopolymerization has been witnessed in the past years. Highly efficient and multifunctional photoinitiators or photoinitiating systems including small molecules, polymers, and nanoassemblies were widely explored for their potential in 3D printing. In this review, recent five main research trends in this field are focused on: i) visible light photoinitiators beyond 405 nm, especially for the ones compatible with white, green, red or even NIR light LEDs, which may facilitate the application of vat photopolymerization such as SLA and DLP in biomedicine due to the low-energy excitation; ii) RAFT photoinitiating systems for living 3D printing, which enabled the post-functionalization of 3D printed objects in a controlled or "living" manner; iii) molecular photoswitches for functional 3D printing, especially multimaterial fabrication and volumetric printing that brought new scope to the field of vat photopolymerization; iv) polymeric photoinitiators that can tackle the solubility/compatibility issue of small molecules, increase the initiation efficiency and simultaneously enhance the crosslinking density; v) nanoparticular systems or upconversion nanosystems for visible-to-NIR light photopolymerization using conventional UV/blue light photoinitiators, which enabled high resolution hydrogel fabrication or even noninvasive in vivo printing.

Although many exciting results have been achieved in vat photopolymerization 3D printing using advanced photoinitiators, numerous challenges and opportunities remain in both molecular design and physical/biological characterization for their applications:

i. The white or green-to-NIR light photoinitiating systems that allow rapid and high-resolution 3D printing are still rare compared to blue/UV light systems. Systematic investigation of various promising organic photoredox dyes, including both commercial dyes and newly synthesized ones which were not used in 3D printing, would be appealing. Machine learning could be an invaluable tool for performance prediction based on the reported data,[109,110] and thus facilitate the selection of most interesting photoinitiators in particular tricomponent systems with minimal experimental work.
ii. Despite the advantage of RAFT-mediated 3D printing, its print speed and resolution are still limited if commercial photoinitiators (e.g., TPO) are not added. Therefore, more efficient RAFT systems insensitive to oxygen and water are to be developed, especially for visible light 3D printing (e.g., green light). Although some preliminary results have been observed,[111] more detailed comparison between RAFT system and conventional 3D printing could be done regarding the mechanical properties and crosslinking networks of the printed products, to further understand the structure–property relationships. On the other hand, other photocontrolled polymerization techniques (e.g., atom transfer radical polymerization, ATRP) could be also explored with a different perspective in terms of chemistry.
iii. The scope of suitable materials is relatively small for the multimaterial 3D printing using photoswitches compared with the air jet-based technique, as only the combination of epoxides and acrylates was tested. In parallel, only several commercial monomers (e.g., PETA and diurethane dimethacrylate) have been employed in photoswitch-based linear volumetric printing. More materials such as biodegradable photopolymers (e.g., polyester acrylates) that can have practical impact (e.g., bioresorbable device fabrication) may be worth investigating in addition to the design of new photoswitchable molecules.
iv. In contrary to the large amount of polymeric photoinitiators developed for non-3D printing purpose, there are only very few examples used in SLA and DLP. A large space in biocompatible and biodegradable macrophotoinitiators for 3D printing remains unexplored regarding the rapid progress of vat photopolymerization in biomedical applications. Bifunctional photoinitiators bearing polymerizable groups[112] could also be designed to enhance the crosslinking network for specific applications. In addition, polymer-based charge transfer systems[85,113] may be worth evaluating for their photoinitiating ability.

 © 2022 The Authors. Macromolecular Rapid Communications published by Wiley-VCH GmbH

v. Customized nanocomposites with different functions (e.g., drug delivery or medical imaging) may be conveniently manufactured by using the corresponding nanophotoinitiators in combination with other functional photopolymers (e.g., drug- or fluorophore-conjugated polymers[114,115]). On the other hand, upconversion nanoparticle-assisted NIR 3D printing is still in its infancy, which still requires parameter optimization for more general applications, for example lowering light intensity, reducing nanoparticle concentration and improving printing resolution. New triplet fusion upconversion systems may be further explored by combining a wide range of molecular annihilators and sensitizers as well as highly efficient visible light photoinitiators.

In general, the multicomponent photoinitiating systems were rarely evaluated for their biocompatibility which, however, is highly important for their application in biomedicine. In particular, the electron donors or acceptors were sometimes used with even higher concentration than the dye molecules. The residues in the 3D printed products may bring non-negligible cytotoxicity to the living cell-related environment. Therefore, systematic in vitro characterizations would be important for the real application of these advanced photoinitiating systems. Overall, the exploration of novel photoinitiators or photoinitiating systems is believed to be an essential part to further push the boundaries of photopolymerization 3D printing for broad applications, in alliance with the development of new printing techniques and the design of photopolymerizable materials.

Acknowledgements

The Swiss National Science Foundation is acknowledged for financial support (Sinergia No. 177178 and Spark No. 190313).

Open access funding provided by Eidgenossische Technische Hochschule Zurich.

Conflict of Interest

The author declares no conflict of interest.

Keywords

3D printing, digital light processing, photoinitiating systems, photoinitiators, stereolithography, vat photopolymerization, volumetric printing

Received: February 28, 2022
Revised: April 14, 2022
Published online: May 26, 2022

[1] M. Schaffner, P. A. Rühs, F. Coulter, S. Kilcher, A. R. Studart, *Sci. Adv.* **2017**, *3*, eaao6804.
[2] J. Koffler, W. Zhu, X. Qu, O. Platoshyn, J. N. Dulin, J. Brock, L. Graham, P. Lu, J. Sakamoto, M. Marsala, S. Chen, M. H. Tuszynski, *Nat. Med.* **2019**, *25*, 263.
[3] J. U. Lind, T. A. Busbee, A. D. Valentine, F. S. Pasqualini, H. Yuan, M. Yadid, S.-J. Park, A. Kotikian, A. P. Nesmith, P. H. Campbell, J. J. Vlassak, J. A. Lewis, K. K. Parker, *Nat. Mater.* **2017**, *16*, 303.
[4] C. Yu, J. Schimelman, P. Wang, K. L. Miller, X. Ma, S. You, J. Guan, B. Sun, W. Zhu, S. Chen, *Chem. Rev.* **2020**, *120*, 10695.
[5] A. Bagheri, J. Jin, *ACS Appl. Polym. Mater.* **2019**, *1*, 593.
[6] X. Xu, A. Awad, P. Robles-Martinez, S. Gaisford, A. Goyanes, A. W. Basit, *J. Controlled Release* **2021**, *329*, 743.
[7] F. P. W. Melchels, J. Feijen, D. W. Grijpma, *Biomaterials* **2010**, *31*, 6121.
[8] R. J. Mondschein, A. Kanitkar, C. B. Williams, S. S. Verbridge, T. E. Long, *Biomaterials* **2017**, *140*, 170.
[9] S. H. Kim, Y. K. Yeon, J. M. Lee, J. R. Chao, Y. J. Lee, Y. B. Seo, M.. T. Sultan, O. J. Lee, J. S. Lee, S.-I. Yoon, I.-S. Hong, G. Khang, S. J. Lee, J. J. Yoo, C. H. Park, *Nat. Commun.* **2018**, *9*, 1620.
[10] X. Kuang, J. Wu, K. Chen, Z. Zhao, Z. Ding, F. Hu, D. Fang, H. J. Qi, *Sci. Adv.* **2019**, *5*, eaav5790.
[11] J. R. Tumbleston, D. Shirvanyants, N. Ermoshkin, R. Janusziewicz, A. R. Johnson, D. Kelly, K. Chen, R. Pinschmidt, J. P. Rolland, A. Ermoshkin, E. T. Samulski, J. M. Desimone, *Science* **2015**, *347*, 1349.
[12] H. J. Oh, M. S. Aboian, M. Y. J. Yi, J. A. Maslyn, W. S. Loo, X.i Jiang, D. Y. Parkinson, M. W. Wilson, T. Moore, C. R. Yee, G. R. Robbins, F. M. Barth, J. M. Desimone, S. W. Hetts, N. P. Balsara, *ACS Cent. Sci.* **2019**, *5*, 419.
[13] B. Grigoryan, S. J. Paulsen, D. C. Corbett, D. W. Sazer, C. L. Fortin, A. J. Zaita, P. T. Greenfield, N. J. Calafat, J. P. Gounley, A. H. Ta, F. Johansson, A. Randles, J. E. Rosenkrantz, J. D. Louis-Rosenberg, P. A. Galie, K. R. Stevens, J. S. Miller, *Science* **2019**, *364*, 458.
[14] R. Gauvin, Y.-C. Chen, J. W. Lee, P. Soman, P. Zorlutuna, J. W. Nichol, H. Bae, S. Chen, A. Khademhosseini, *Biomaterials* **2012**, *33*, 3824.
[15] N. Paunović, Y. Bao, F. B. Coulter, K. Masania, A. K. Geks, K. Klein, A. Rafsanjani, J. Cadalbert, P. W. Kronen, N. Kleger, A. Karol, Z. Luo, F. Rüber, D. Brambilla, B. Von Rechenberg, D. Franzen, A. R. Studart, J.-C. Leroux, *Sci. Adv.* **2021**, *7*, abe9499.
[16] N. Maity, N. Mansour, P. Chakraborty, D. Bychenko, E. Gazit, D. Cohn, *Adv. Funct. Mater.* **2021**, *31*, 2108436.
[17] E. Sachyani Keneth, A. Kamyshny, M. Totaro, L. Beccai, S. Magdassi, *Adv. Mater.* **2021**, *33*, 2003387.
[18] D. K. Patel, A. H. Sakhaei, M. Layani, B. Zhang, Q.i Ge, S. Magdassi, *Adv. Mater.* **2017**, *29*, 1606000.
[19] A. Della Bona, V. Cantelli, V. T. Britto, K. F. Collares, J. W. Stansbury, *Dent. Mater.* **2021**, *37*, 336.
[20] M. Dehurtevent, L. Robberecht, J. -. C. Hornez, A. Thuault, E. Deveaux, P. Béhin, *Dent. Mater.* **2017**, *33*, 477.
[21] A. K. Au, W. Huynh, L. F. Horowitz, A. Folch, *Angew. Chem., Int. Ed.* **2016**, *55*, 3862.
[22] N. Bhattacharjee, C. Parra-Cabrera, Y. T. Kim, A. P. Kuo, A. Folch, *Adv. Mater.* **2018**, *30*, 1800001.
[23] S. Borandeh, B. Van Bochove, A. Teotia, J. Seppälä, *Adv. Drug Delivery Rev.* **2021**, *173*, 349.
[24] M. Shusteff, A. E. M. Browar, B. E. Kelly, J. Henriksson, T. H. Weisgraber, R. M. Panas, N. X. Fang, C. M. Spadaccini, *Sci. Adv.* **2017**, *3*, eaao5496.
[25] B. E. Kelly, I. Bhattacharya, H. Heidari, M. Shusteff, C. M. Spadaccini, H. K. Taylor, *Science* **2019**, *363*, 1075.
[26] D. Loterie, P. Delrot, C. Moser, *Nat. Commun.* **2020**, *11*, 852.
[27] M. Regehly, Y. Garmshausen, M. Reuter, N. F. König, E. Israel, D. P. Kelly, C.-Y. Chou, K. Koch, B. Asfari, S. Hecht, *Nature* **2020**, *588*, 620.
[28] a) E. Andrzejewska, *Prog. Polym. Sci.* **2001**, *26*, 605; b) S. Shi, C. Croutxé-Barghorn, X. Allonas, *Prog. Polym. Sci.* **2017**, *65*, 1; c) G. Oster, N.-L. Yang, *Chem. Rev.* **1968**, *68*, 125; d) A. B. Scranton, C. N. Bowman, R. W. Peiffer, *Photopolymerization: Fundamentals and Applications*, ACS Symposium Series, Vol. *673*, American Chemical Society, Washington, DC **1997**.
[29] a) P. Garra, J. P. Fouassier, S. Lakhdar, Y. Yagci, J. Lalevée, *Prog. Polym. Sci.* **2020**, *107*, 101277; b) P. Xiao, J. Zhang, F. Dumur, M. A. Tehfe, F. Morlet-Savary, B. Graff, D. Gigmes, J. P. Fouassier, J. Lalevée, *Prog. Polym. Sci.* **2015**, *41*, 32.

 © 2022 The Authors. Macromolecular Rapid Communications published by Wiley-VCH GmbH

[30] J. Zhang, P. Xiao, *Polym. Chem.* **2018**, *9*, 1530.
[31] a) D. Zhu, J. Zhang, J. Lalevée, P. Xiao, in *3D Printing with Light*, (Eds: P. Xiao, J. Zhang), Walter de Gruyter, Berlin **2021**, Ch. 1; b) W. Tomal, J. Ortyl, *Polymers* **2020**, *12*, 1073; c) Y. Zhang, Y. Xu, A. Simon-Masseron, J. Lalevée, *Chem. Soc. Rev.* **2021**, *50*, 3824.
[32] D. Ahn, L. M. Stevens, K. Zhou, Z. A. Page, *ACS Cent. Sci.* **2020**, *6*, 1555.
[33] N. D. Dolinski, Z. A. Page, E. B. Callaway, F. Eisenreich, R. V. Garcia, R. Chavez, D. P. Bothman, S. Hecht, F. W. Zok, C. J. Hawker, *Adv. Mater.* **2018**, *30*, 1800364;
[34] Z. Zhang, N. Corrigan, A. Bagheri, J. Jin, C. Boyer, *Angew. Chem., Int. Ed.* **2019**, *58*, 17954.
[35] a) J. Wang, S. Stanic, A. A. Altun, M. Schwentenwein, K. Dietliker, L.u Jin, J. Stampfl, S. Baudis, R. Liska, H. Grützmacher, *Chem. Commun.* **2018**, *54*, 920; b) S. N. Anindita, R. Conti, D. Zauchner, N. Paunović, W. Qiu, M. G. Buzhor, Z. Luo, R. Müller, H. Grützmacher, X.-H. Qin, J.-C. Leroux, Y. Bao, *ChemRxiv* **2022**, https://doi.org/10.26434/chemrxiv-2022-tklpl.
[36] M. Sandmeier, N. Paunović, R. Conti, L. Hofmann, J. Wang, Z. Luo, K. Masania, N. Wu, N. Kleger, F. B. Coulter, A. R. Studart, H. Grützmacher, J.-C. Leroux, Y. Bao, *Macromolecules* **2021**, *54*, 7830.
[37] A. A. Pawar, G. Saada, I. Cooperstein, L. Larush, J. A. Jackman, S. R. Tabaei, N.-J. Cho, S. Magdassi, *Sci. Adv.* **2016**, *2*, e1501381.
[38] J. Wang, A. Chiappone, I. Roppolo, F. Shao, E. Fantino, M. Lorusso, D. Rentsch, K. Dietliker, C. F. Pirri, H. Grützmacher, *Angew. Chem., Int. Ed.* **2018**, *57*, 2353.
[39] a) J. Wang, *Ph.D. Thesis*, ETH Zurich, **2017**; b) B. Ganster, U. K. Fischer, N. Moszner, R. Liska, *Macromol. Rapid Commun.* **2008**, *29*, 57.
[40] C. Dietlin, S. Schweizer, P. Xiao, J. Zhang, F. Morlet-Savary, B. Graff, J.-P. Fouassier, J. Lalevée, *Polym. Chem.* **2015**, *6*, 3895;
[41] A. Al Mousawi, C. Poriel, F. Dumur, J. Toufaily, T. Hamieh, J. P. Fouassier, J. Lalevée, *Macromolecules* **2017**, *50*, 746.
[42] Z. Wang, H. Kumar, Z. Tian, X. Jin, J. F. Holzman, F. Menard, K. Kim, *ACS Appl. Mater. Interfaces* **2018**, *10*, 26859.
[43] M. Chen, M. Zhong, J. A. Johnson, *Chem. Rev.* **2016**, *116*, 10167.
[44] S. Dadashi-Silab, S. Doran, Y. Yagci, *Chem. Rev.* **2016**, *116*, 10212.
[45] X. Pan, M. A. Tasdelen, J. Laun, T. Junkers, Y. Yagci, K. Matyjaszewski, *Prog. Polym. Sci.* **2016**, *62*, 73.
[46] B. Steyrer, P. Neubauer, R. Liska, J. Stampfl, *Materials* **2017**, *10*, 1445.
[47] a) J. Zhang, F. Dumur, P.u Xiao, B. Graff, D. Bardelang, D. Gigmes, J. P. Fouassier, J. Lalevée, *Macromolecules* **2015**, *48*, 2054; b) A. Al Mousawi, P. Garra, X. Sallenave, F. Dumur, J. Toufaily, T. Hamieh, B. Graff, D. Gigmes, J. P. Fouassier, J. Lalevée, *Macromolecules* **2018**, *51*, 1811.
[48] Z. Wang, R. Abdulla, B. Parker, R. Samanipour, S. Ghosh, K. Kim, *Biofabrication* **2015**, *7*, 045009.
[49] C.s Bahney, T.j Lujan, C.w Hsu, M. Bottlang, J.l West, B. Johnstone, *Eur. Cells Mater.* **2011**, *22*, 43.
[50] K. S. Lim, B. S. Schon, N. V. Mekhileri, G. C. J. Brown, C. M. Chia, S. Prabakar, G. J. Hooper, T. B. F. Woodfield, *ACS Biomater. Sci. Eng.* **2016**, *2*, 1752.
[51] S. Bertlein, G. Brown, K. S. Lim, T. Jungst, T. Boeck, T. Blunk, J. Tessmar, G. J. Hooper, T. B. F. Woodfield, J. Groll, *Adv. Mater.* **2017**, *29*, 1703404.
[52] W. Li, M. Wang, L. S. Mille, J. A. Robledo Lara, V. Huerta, T. Uribe Velázquez, F. Cheng, H. Li, J. Gong, T. Ching, C. A. Murphy, A. Lesha, S. Hassan, T. B. F. Woodfield, K. S. Lim, Y. S. Zhang, *Adv. Mater.* **2021**, *33*, 2102153.
[53] X. Xu, A. Seijo-Rabina, A. Awad, C. Rial, S. Gaisford, A. W. Basit, A. Goyanes, *Int. J. Pharm.* **2021**, *609*, 121199.
[54] K. Kowsari, W. Lee, S.-S. Yoo, N. X. Fang, *iScience* **2021**, *24*, 103372.
[55] a) J. Zhang, K. Launay, N. S. Hill, D. Zhu, N. Cox, J. Langley, J. Lalevée, M. H. Stenzel, M. L. Coote, P. Xiao, *Macromolecules* **2018**, *51*, 10104; b) G. Wang, N. S. Hill, D.i Zhu, P.u Xiao, M. L. Coote, M. H. Stenzel, *ACS Appl. Polym. Mater.* **2019**, *1*, 1129; c) G. Wang, C. Ma, T. Hu, T. Wang, *3D Print. Addit. Manuf.* 2021, https://doi.org/10.1089/3dp.2021.0204.
[56] A. Stafford, D. Ahn, E. K. Raulerson, K. -. Y. Chung, K. Sun, D. M. Cadena, E. M. Forrister, S. R. Yost, S. T. Roberts, Z. A. Page, *J. Am. Chem. Soc.* **2020**, *142*, 14733.
[57] L. M. Stevens, C. Tagnon, Z. A. Page, *ACS Appl. Mater. Interfaces* **2022**, https://doi.org/10.1021/acsami.1c22046.
[58] B. Metral, A. Bischoff, C. Ley, A. Ibrahim, X. Allonas, *ChemPhotoChem* **2019**, *3*, 1109.
[59] X. Zhao, Y.e Zhao, M.-D.e Li, Z.'A.n Li, H. Peng, T. Xie, X. Xie, *Nat. Commun.* **2021**, *12*, 2873.
[60] A. Bagheri, K. E. Engel, C. W. A. Bainbridge, J. Xu, C. Boyer, J. Jin, *Polym. Chem.* **2020**, *11*, 641.
[61] A. Bagheri, C. W. A. Bainbridge, K. E. Engel, G. G. Qiao, J. Xu, C. Boyer, J. Jin, *ACS Appl. Polym. Mater.* **2020**, *2*, 782.
[62] K. Lee, N. Corrigan, C. Boyer, *Angew. Chem., Int. Ed.* **2021**, *60*, 8839.
[63] Z. Zhang, N. Corrigan, C. Boyer, *Angew. Chem., Int. Ed.* **2022**, 61, e202114111.
[64] X. Shi, J. Zhang, N. Corrigan, C. Boyer, *Polym. Chem.* **2022**, *13*, 44.
[65] V. A. Bobrin, K. Lee, J. Zhang, N. Corrigan, C. Boyer, *Adv. Mater.* **2022**, *34*, 2107643.
[66] A. Bagheri, H. Ling, C. W. A. Bainbridge, J. Jin, *ACS Appl. Polym. Mater.* **2021**, *3*, 2921.
[67] B. Zhao, J. Li, X. Pan, Z. Zhang, G. Jin, J. Zhu, *ACS Macro Lett.* **2021**, *10*, 1315.
[68] B. Zhao, J. Li, Y. Xiu, X. Pan, Z. Zhang, J. Zhu, *Macromolecules* **2022**, *55*, 1620.
[69] J. R. Hemmer, S. O. Poelma, N. Treat, Z. A. Page, N. D. Dolinski, Y. J. Diaz, W. Tomlinson, K. D. Clark, J. P. Hooper, C. Hawker, J. Read De Alaniz, *J. Am. Chem. Soc.* **2016**, *138*, 13960.
[70] M. Gernhardt, E. Blasco, M. Hippler, J. Blinco, M. Bastmeyer, M. Wegener, H. Frisch, C. Barner-Kowollik, *Adv. Mater.* **2019**, *31*, 1901269.
[71] S. Ulrich, X. Wang, M. Rottmar, R. M. Rossi, B. J. Nelson, N. Bruns, R. Müller, K. Maniura-Weber, X.-. H. Qin, L. F. Boesel, *Small* **2021**, *17*, 2101337.
[72] N. D. Dolinski, E. B. Callaway, C. S. Sample, L. F. Gockowski, R. Chavez, Z. A. Page, F. Eisenreich, S. Hecht, M. T. Valentine, F. W. Zok, C. J. Hawker, *ACS Appl. Mater. Interfaces* **2021**, *13*, 22065.
[73] M. P. De Beer, H. L. Van Der Laan, M. A. Cole, R. J. Whelan, M. A. Burns, T. F. Scott, *Sci. Adv.* **2019**, *5*, eaau8723.
[74] H. L. Van Der Laan, M. A. Burns, T. F. Scott, *ACS Macro Lett.* **2019**, *8*, 899.
[75] J. J. Schwartz, A. J. Boydston, *Nat. Commun.* **2019**, *10*, 791.
[76] J. Zhou, X. Allonas, A. Ibrahim, X. Liu, *Prog. Polym. Sci.* **2019**, *99*, 101165.
[77] a) H. Wang, B. Zhang, J. Zhang, X. He, F. Liu, J. Cui, Z. Lu, G. Hu, J. Yang, Z. Zhou, R. Wang, X. Hou, L. Ma, P. Ren, Q. Ge, P. Li, W. Huang, *ACS Appl. Mater. Interfaces* **2021**, *13*, 55507;. b) D. Shin, J. Hyun, *J. Ind. Eng. Chem.* **2021**, *95*, 126; c) B. D. Fairbanks, M. P. Schwartz, C. N. Bowman, K. S. Anseth, *Biomaterials* **2009**, *30*, 6702;. d) T. Majima, W. Schnabel, W. Weber, *Makromol. Chem.* **1991**, *192*, 2307; e) C. M. Q. Le, T. Petitory, X. Wu, A. Spangenberg, J. Ortyl, M. Galek, L. Infante, H. Thérien-Aubin, A. Chemtob, *Macromol. Chem. Phys.* **2021**, *222*, 2100217.
[78] C. Xu, R. A. D. Arancon, J. Labidi, R. Luque, *Chem. Soc. Rev.* **2014**, *43*, 7485.
[79] a) Y. Liu, X. Huang, K. Han, Y. Dai, X. Zhang, Y. Zhao, *ACS Sustainable Chem. Eng.* **2019**, *7*, 4004; b) J. T. Sutton, K. Rajan, D. P. Harper, S. C. Chmely, *ACS Appl. Mater. Interfaces* **2018**, *10*, 36456.
[80] X. Zhang, S. Keck, Y. Qian, S. Baudis, Y. Zhao, *ACS Sustainable Chem. Eng.* **2020**, *8*, 10959.
[81] a) Y. Bao, N. Paunović, J.-C. Leroux, *Adv. Funct. Mater.* **2022**, *32*, 2109864; b) N. Paunović, J.- C. Leroux, Y. Bao, *Polym. Chem.* **2022**, *13*, 2271.

 © 2022 The Authors. Macromolecular Rapid Communications published by Wiley-VCH GmbH

[82] A. Cosola, R. Conti, V. K. Rana, M. Sangermano, A. Chiappone, J. Levalois-Grützmacher, H. Grützmacher, *Chem. Commun.* **2020**, *56*, 4828.
[83] A. Cosola, M. Sangermano, D. Terenziani, R. Conti, M. Messori, H. Grützmacher, C. F. Pirri, A. Chiappone, *Appl. Mater. Today* **2021**, *23*, 101060.
[84] Y. Han, F. Wang, C. Y. Lim, H. Chi, D. Chen, F. Wang, X. Jiao, *ACS Appl. Mater. Interfaces* **2017**, *9*, 32418.
[85] A. Baralle, P. Garra, B. Graff, F. Morlet-Savary, C. Dietlin, J. P. Fouassier, S. Lakhdar, J. Lalevée, *Macromolecules* **2019**, *52*, 3448.
[86] M. Tromayer, P. Gruber, M. Markovic, A. Rosspeintner, E. Vauthey, H. Redl, A. Ovsianikov, R. Liska, *Polym. Chem.* **2017**, *8*, 451.
[87] S. Mura, J. Nicolas, P. Couvreur, *Nat. Mater.* **2013**, *12*, 991.
[88] G. Chen, I. Roy, C. Yang, P. N. Prasad, *Chem. Rev.* **2016**, *116*, 2826.
[89] S. Matoori, Y. Bao, A. Schmidt, E. J. Fischer, R. Ochoa-Sanchez, M. Tremblay, M. M. Oliveira, C. F. Rose, J.-C. Leroux, *Small* **2019**, *15*, 1902347.
[90] J. Dos Santos, R. S. Oliveira, T. V. Oliveira, M. C. Velho, M. V. Konrad, G. S. Da Silva, M. Deon, R. C. R. Beck, *Adv. Funct. Mater.* **2021**, *31*, 2009691.
[91] U. Kolczak, G. Rist, K. Dietliker, J. Wirz, *J. Am. Chem. Soc.* **1996**, *118*, 6477.
[92] N. Waiskopf, Y. Ben-Shahar, M. Galchenko, I. Carmel, G. Moshitzky, H. Soreq, U. Banin, *Nano Lett.* **2016**, *16*, 4266.
[93] A. A. Pawar, S. Halivni, N. Waiskopf, Y. Ben-Shahar, M. Soreni-Harari, S. Bergbreiter, U. Banin, S. Magdassi, *Nano Lett.* **2017**, *17*, 4497.
[94] S. Benedikt, J. Wang, M. Markovic, N. Moszner, K. Dietliker, A. Ovsianikov, H. Grützmacher, R. Liska, *J. Polym. Sci., Part A: Polym. Chem.* **2016**, *54*, 473.
[95] Y. Zhu, E. Ramadani, E. Egap, *Polym. Chem.* **2021**, *12*, 5106.
[96] W. Tomal, T. Świergosz, M. Pilch, W. Kasprzyk, J. Ortyl, *Polym. Chem.* **2021**, *12*, 3661.
[97] a) J. George, S. N. Sabapathi, *Nanotechnol. Sci. Appl.* **2015**, *8*, 45; b) M. Carrola, A. Asadi, H. Zhang, D. G. Papageorgiou, E. Bilotti, H. Koerner, *Adv. Funct. Mater.* **2021**, *31*, 2103334.
[98] S. Wen, J. Zhou, K. Zheng, A. Bednarkiewicz, X. Liu, D. Jin, *Nat. Commun.* **2018**, *9*, 2415.
[99] Z. Chen, S. He, H.-J. Butt, S.i Wu, *Adv. Mater.* **2015**, *27*, 2203.
[100] V. V. Rocheva, A. V. Koroleva, A. G. Savelyev, K. V. Khaydukov, A. N. Generalova, A. V. Nechaev, A. E. Guller, V. A. Semchishen, B. N. Chichkov, E. V. Khaydukov, *Sci. Rep.* **2018**, *8*, 3663.
[101] S. N. Sanders, T. H. Schloemer, M. K. Gangishetty, D. Anderson, M. Seitz, A. O. Gallegos, R. C. Stokes, D. N. Congreve, *Nature* **2022**, *604*, 474.
[102] J. Méndez-Ramos, J. C. Ruiz-Morales, P. Acosta-Mora, N. M. Khaidukov, *J. Mater. Chem. C* **2016**, *4*, 801.
[103] R. Liu, H. Chen, Z. Li, F. Shi, X. Liu, *Polym. Chem.* **2016**, *7*, 2457.
[104] A. Stepuk, D. Mohn, R. N. Grass, M. Zehnder, K. W. Krämer, F. Pellé, A. Ferrier, W. J. Stark, *Dent. Mater.* **2012**, *28*, 304.
[105] Y. Chen, J. Zhang, X. Liu, S. Wang, J. Tao, Y. Huang, W. Wu, Y. Li, K. Zhou, X. Wei, S. Chen, X. Li, X. Xu, L. Cardon, Z. Qian, M. Gou, *Sci. Adv.* **2020**, *6*, eaba7406.
[106] J. Zhu, Q. Zhang, T. Yang, Y.u Liu, R. Liu, *Nat. Commun.* **2020**, *11*, 3462.
[107] X. Zou, J. Zhu, Y.e Zhu, Y. Yagci, R. Liu, *ACS Appl. Mater. Interfaces* **2020**, *12*, 58287.
[108] M. Panzer, J. R. Tumbleston, (Carbon Inc), US11117316B2, **2017**.
[109] G. D. Goh, S. L. Sing, W. Y. Yeong, *Artif. Intell. Rev.* **2021**, *54*, 63.
[110] M. Elbadawi, L. E. Mccoubrey, F. K. H. Gavins, J. J. Ong, A. Goyanes, S. Gaisford, A. W. Basit, *Trends Pharmacol. Sci.* **2021**, *42*, 745.
[111] X. Shi, J. Zhang, N. Corrigan, C. Boyer, *Mater. Chem. Front.* **2021**, *5*, 2271.
[112] W. Qiu, J. Zhu, K. Dietliker, Z. Li, *ChemPhotoChem* **2020**, *4*, 5296.
[113] S. Ye, T. Tian, A. J. Christofferson, S. Erikson, J. Jagielski, Z. Luo, S. Kumar, C.-J. Shih, J.-C. Leroux, Y. Bao, *Sci. Adv.* **2021**, *7*, eabd1794.
[114] Y. Bao, J. Nicolas, *Polym. Chem.* **2017**, *8*, 5174.
[115] Y. Bao, H. De Keersmaecker, S. Corneillie, F. Yu, H. Mizuno, G. Zhang, J. Hofkens, B. Mendrek, A. Kowalczuk, M. Smet, *Chem. Mater.* **2015**, *27*, 3450.

Yinyin Bao is a group leader in the Institute of Pharmaceutical Sciences at ETH Zürich, Switzerland. Dr. Bao received his Ph.D. degree in polymer chemistry from the University of Science and Technology of China in 2012. Then he completed postdoctoral research at KU Leuven (Belgium), and in 2014 became a Marie Curie IntraEuropean Fellow of CNRS at the University of Paris Sud (France). In 2016 he joined the group of Prof. Jean-Christophe Leroux, and he was promoted to a senior scientist position in late 2018. His research interests remain light-emitting materials, drug delivery, and 3D printing.

 © 2022 The Authors. Macromolecular Rapid Communications published by Wiley-VCH GmbH